Research on Engineering Structures & Materials
www.jresm.org
Research Group

Research Article

Development and characterization of carbon nanotube/green titania as potential hybrid nanofiller in nanofluid for machining carbon fiber reinforced plastics

Sunday Albert Lawal[1,a], Rasaq Olawale Medupin[2,b,*], Victor Chiagozie Nwachukwu[1,c], Uzoma Gregory Okoro[1,d], Oyewole Adedipe[1,e], Joseph Abutu[3,f], Benjamin I. Attah[4,g], Jimoh Oladejo Tijani[5,h], Ambali Saka Abdulkareem[6,i]

[1]*Dept. of Mechanical Eng., Federal University of Technology, Minna, 920101, Nigeria*
[2]*Dept. of Mechanical Eng., Federal University Lokoja, Lokoja, 260101, Nigeria*
[3]*Dept. of Mechanical Eng., Taraba State University, Jalingo, 660213, Nigeria*
[4]*Dept. of Mechanical Eng., African University of Science and Technology, Abuja, 900107, Nigeria*
[5]*Dept. of Chemistry, Federal University of Technology, Minna, 920101, Nigeria*
[6]*Dept. of Chemical Engineering, Federal University of Technology, Minna, 920101, Nigeria*

Article Info

Article History:

Received 15 Aug 2024
Accepted 27 Nov 2024

Keywords:

Synthesis;
Characterization;
Cabon nanotube;
Green titania;
CFRPs;
Nanocomposites

Abstract

In the industry, removing heat from cutting zones during machining presents a major challenge. Consequently, there is increased demand for reasonably priced and environmentally safe cooling agents during carbon fiber reinforced polymers (CFRPs) machining for high-performance applications. This work synthesized and characterized green titania (TiO_2) and carbon nanotubes (CNTs) to create TiO_2/CNTs nanocomposites (NCs) with varying proportions (9:1, 7:3, and 5:5). To investigate the NCs' stability as potential fillers in base oils for creating nanofluids for machining carbon fiber reinforced plastics (CFRPs), a variety of analytical techniques was used to characterize them, including Brunauer-Emmett-Teller (BET), high resolution SEM/EDS, high resolution TEM, XRD, and FTIR. The FTIR spectra of the NCs indicate absorption peaks that are consistent with C=C and Ti-O bonds, generating peaks allocated to Ti-O-C and C-O bonds. Because primary peaks of CNTs and TiO_2 overlap, the peaks attributed to CNTs are hardly visible and those of anatase are easily identifiable. Due to their larger surface area, pore volume, and stability as a nanosuspension, TiO_2/CNTs (5:5) offers significant benefits over other NCs for heat removal: here lies the novelty of this research article utilizing green titania. The challenges associated with uncontrollable agglomeration of individual NCs are addressed by these hybrid NCs. Thus, it is concluded that TiO_2/CNTs NCs are potential reinforcing fillers in base oils for machining.

1. Introduction

For many years, carbon fiber reinforced polymers, or CFRPs, have been recognized as essential materials for a wide range of engineering applications. Their current prominence in manufacturing technology is a result of their exceptional performance in the fields of aircraft, luxury consumer goods, and national defense [1]. Their enhanced mechanical qualities and increased competitiveness as high-performance materials in automotive and structural applications are attributed to the reinforcing strength of carbon fibers. Nevertheless, as a material with comparative

*Corresponding author: rasaq.medupin@fulokoja.edu.ng
[a]orcid.org/0000-0002-2818-9146; [b]orcid.org/0000-0002-9822-041X; [c]orcid.org/0009-0004-7076-1283; [d]orcid.org/0000-0002-4798-1876; [e]orcid.org/0000-0002-1840-7031; [f]orcid.org/0000-0003-1494-9201; [g]orcid.org/0009-0008-6877-7648; [h]orcid.org/0000-0002-1707-0078; [i]orcid.org/0000-0003-0049-3186
DOI: http://dx.doi.org/10.17515/resm2024.399ma0815rs

benefits, CFRP machining has not gotten nearly as much attention as it should until lately [2,3]. Scholars who have examined the machining of CFRPs using traditional cutting fluids have criticized the difficulties involved and have called for additional research to unravel the uncharted waters [4-6]. It has been demonstrated that the majority of conventional cutting fluids have continually failed to maintain their relevance in the present efforts to comply with SDG #12 of the United Nations (UN) on responsible consumption and production.

The degree of process success regarding tool life, cutting speed, and surface smoothness is impacted by the prompt and simple removal of heat from cutting zones during machining [7]. In pursuit of sustainable green manufacturing, Lawal et al. [8] reported on the preference for bio-oil-based cutting fluids to offer answers to various health problems connected with synthetic cutting fluids. While both vegetable and synthetic oils serve as effective temporary coolants during machining, the possibility of a chemical imbalance initiating corrosion process raises many concerns in today's eco-aware society [9]. Because of this, nanofluids are now being developed to use the quality and huge surface areas offered by nanoparticles (NPs) to address difficulties related to rapid heat removal from the tool/workpiece interface. This is expected to speed up heat evacuation and assist in lowering the amount of fluid required for a certain machining procedure [10]. Environmental pollution is effectively addressed in the same way that cost is adequately managed since both the volume of cutting fluids required and the volume released into the surrounding environment after usage are significantly decreased [11-13]. The Minimum Quantity Lubrication (MQL) technique was developed to further optimize machining settings in accordance with this principle [14]. MQL is a more economical and environmentally beneficial solution than flooding and the use of dry cutting fluid [15]. In the context of sustainable manufacturing, this machining procedure is congruent with more ethical and cleaner production.

But more recently, a better method of carrying out the complementary tasks of lubrication and heat removal during machining has been introduced, and the scientific community is now paying greater attention to it [16]. The fluid lubricates the cutting interface, and the nanofillers transfer heat away from the cutting zone, resulting in a smooth and quick machining process that improves surface finish and prolongs tool life [17,18]. This is referred to as nMQL, or nanofluid-MQL. In a recent study, Kumar et al. [19] referred to nMQL as the novel chapter in sustainable machining. Low cutting forces are produced by the method of spraying nanofluid mist over the tool-work contact during machining, which changes, sliding into rolling friction between the tool pieces and drastically lowers friction coefficient [20–23]. Assessment research on specific machining parameters under dry and MQL conditions was carried out by Venkatesan et al. [24]. Examination of turning operations under nMQL conditions demonstrates that MQL inhibits the wear mechanism, a typical shortcoming of dry machining. This suggests that using nMQL for sustainable machining of challenging materials for industrial purposes is a positive move [25]. While also investigating the approach, Gao et al. [16] observed that the optimization of the nanofluids under high pressure air flow addresses the challenge of unsatisfactory capability of MQL to transfer of heat in the machining area and advances the lubrication performance of the boundary between the tool and the metals. While acknowledging the likelihood of taking advantage of different properties of NPs to form hybrid nanofluids, Gao et al. [26] submitted that using nMQL technique, processing impairment such as resin covering, multi-fiber block pull-out, and pits can be lowered. Therefore, it can be concluded that nMQL is the future of CFRPs machining.

As good as the nMQL technique appears to be, there are a few issues with the hybrid nanofluid production process. Standard nanosuspension production is still a long-standing procedural difficulty. Because of the van der Waals interactions between individual NPs, Abubakre et al. [27] concurred with one of the previous research studies by Urmi et al. [28] regarding the challenges in achieving lasting equilibrium of hybrid nanofluids, which is a condition for hybrid nanofluid applications. This characteristic of the nanofluids is significant since it enhances the way it behaves thermally when used. As a result, solving the stability problem is essential to performing high-quality machining. According to the literature, if the length of each action is taken into consideration, then external force, stirring, and ultrasonication can be used to disrupt the bonds holding NPs together [29,30]. Therefore, there is still a great vacuum in the literature about the subject of time, particularly when the major goal of the exercise is commercialization.

Therefore, considering how essential NPs can be to achieving exceptional clean machining using the nMQL approach, the procedures involved in producing NPs should receive all the attention they require. In light of this, the objective of this work is to synthesize and characterize high-quality carbon nanotubes (CNTs), green titanium dioxide (TiO_2), and their nanocomposites (NCs) in order to develop hybrid nanofluids that may be used to machine CFRPs.

2. Materials and Methods

2.1. Materials

Chemicals with percentage purity ranging between 95% and 99.98% were used in this work. They were utilized without further purification after being obtained from Sigma Aldrich, a renowned first-class distributor of chemicals in the world. The materials for the studies comprise distilled water, extract from *Terminalia catappa*, sodium hydroxide (NaOH) pellets, methanol (CH_3OH), titanium (IV) isopropoxide ($Ti(OCH(CH_3)_2)_4$, hydrochloric acid (HCl), and sodium dodecyl sulfate (SDS). A few of the tools used are an electric weighing scale, an ultrasonic oscillator (version KQ3200DB), a muffle furnace, a UV-Visible spectrophotometer (UV-1800), a viscometer (NDJ-5S), a 78 HW-1 steady temperature mixer, and other necessities.

2.2. Materials

2.2.1 Production of Green TiO_2 Nanoparticles

Tables 1 and 2 illustrate how an extract of *Terminalia catappa* was used for biosynthesis of titania NPs through the green method. Using a magnetic stirrer, a known volume of titanium isopropoxide was measured and added to a 250 cm^3 beaker holding a predetermined volume of plant extract. Using a solution of NaOH and HCl, the mixture was continuously stirred until the required pH was reached. After that, the mixture was cleaned with deionized water, oven-dried for 12 hours at 105 ^oC, and then calcined for three hours at 450 ^oC. In Fig. 1, the process is depicted in detail.

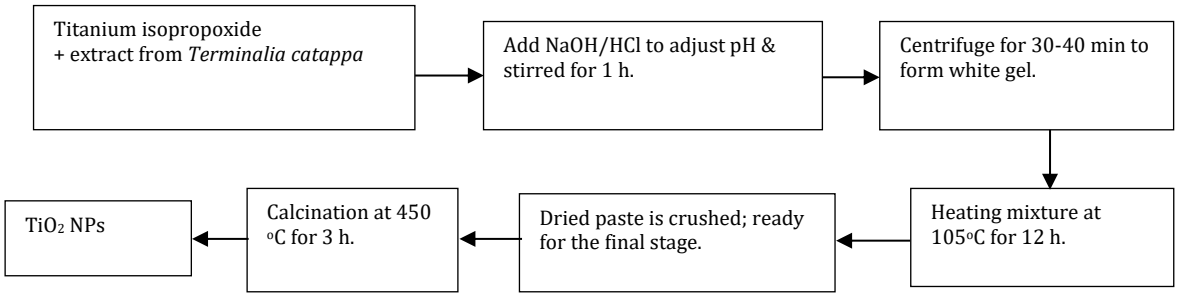

Fig. 1. Procedure for biosynthesis of titania nanoparticles

Table 1. 2^4 Factorial design matrices

Coded value	Volume of extract (cm^3)	Volume of precursor (cm^3)	Mixing time (min)	pH
– Level	50	5	100	2
+ Level	80	8	200	12

Table 2. 2^4 Experimental runs for biosynthesis of titania NPs

Run	Volume of extract (cm^3)	Stirring period (min)	Volume of precursor (cm^3)	pH
1	80	150	8.0	7
2	65	150	5.0	12
3	65	100	6.5	12
4	65	150	8.0	2
5	65	100	5.0	7

6	50	100	6.5	7
7	65	200	6.5	12
8	80	200	6.5	7
9	80	150	6.5	12
10	50	200	6.5	7
11	80	100	6.5	7
12	80	150	6.5	2
13	65	200	6.5	2
14	50	150	8.0	7
15	65	200	8.0	7
16	65	150	6.5	7
17	65	100	8.0	7
18	50	150	5.0	7
19	65	150	5.0	2
20	65	100	6.5	2
21	50	150	6.5	12
22	80	150	5.0	7
23	65	150	8.0	12
24	50	150	6.5	2
25	65	200	5.0	7

2.2.2 Carbon Nanotube Synthesis

After dissolving 14.53 g of Ni and 20.2 g of Fe in 100 ml of distilled water, 10 g of kaolin was introduced. The mix was then stimulated for one hour at 200 rpm using an orbital shaker. Before being decanted, the mixture was allowed to cool and then dried for 12 hours at 120 ^{o}C in the oven. A 150 μm sieve was used to screen and grind the dried mixture. After that, the fine powder (catalyst) was removed from the mixture by calcining it for 16 hours at 500 ^{o}C. In order to prevent agglomeration, which could impair the interaction between the carbon source and the surface mixture, the dried catalyst was then grounded. Subsequently, acetylene, the carbon source, was broken down in a cylindrical quartz reactor that was located horizontally inside a furnace to synthesize carbon nanotubes (CNTs). The reaction temperature, gas flow rates, and heating rate were all properly managed thanks to the electrical controls inside the furnace.

A thin layer of 1.0 g catalyst was applied in an 11 cm by 2.6 cm quartz boat and located midway in the quartz tube. Heat was supplied to the furnace at 10 °C/min, and at the same time, 30 ml of argon (Ar) was fluxed through the system. This was done to guarantee a furnace environment devoid of inert contaminants and to prevent oxidation, both pre- and post-reaction. Argon flow rate was raised to 230 ml/min at 750 ^{o}C. After that, C_2H_2 was added at 150 and 200 ml/min flow rates to start the growth of CNTs. Following a 90-minute reaction time, the C_2H_2 flow was stopped while the furnace cooled to room temperature and argon was continuously passed through the furnace at a rate of 30 milliliters per minute. In order to collect the catalyst and carbon deposit, the boat was removed from the reactor. CNTs yield (%) was computed using Eq (1) as a basis for the relationship.

$$CNTs\ yield(\%) = \frac{W_{product} - W_{catalyst}}{W_{catalyst}} \times 100\ \% \quad (1)$$

Using a 2.0 g measure of CNTs, the support material (kaolin) and the transition metal (Fe-Ni) catalysts were removed from a beaker filled with 200 ml of 3M NaOH solution. After using a magnetic stirrer for three hours, the solution was left to settle. To guarantee a neutral pH, the mix

was then sieved and rinsed in distilled water. After that, it was dried for 24 hours at 120 °C. After being finally sonicated, the CNTs were stored on the shelf for further usage.

2.2.3 Synthesis of Nanocomposites

In a ceramic mortar, a known quantity of CNTs and TiO_2 (TiO_2/CNTs) at various ratios were weighed, and a pestle was used to adequately crush the material. Prior to analysis, the mixes for TiO_2/CNTs at ratios of 9:1, 7:3, and 5:5 were compounded. TiO_2/CNTs at 9:1, 7:3, and 5:5 ratios were disseminated in propanol and sonicated until a homogenous solution was formed in order to create TiO_2/CNTs NCs. Concurrently, the TiO_2 was dissolved in an appropriate solvent and introduced in droplets to the distributed CNTs while sonication was carried out for a prolonged period, immediately succeeded by magnetic stirring. The suspension was poured into a round-bottom flask and heated to 200 °C in an oil bath while being stirred magnetically. The mix was then filtered, left to lose heat naturally to ambient condition, and repeatedly cleaned with ethanol and distilled water. The final composite was then calcined at 550°C and dried at 100°C.

2.3 Characterization of Nanomaterials

2.3.1 X-ray diffraction (XRD)

Bruker AXS D8 Advanced X-ray diffractometer, laden with Cu Kα radiation, was used to examined the phase and crystallite sizes of the nanoparticles. The diffractograms were obtained in the two-theta range of 20 – 90° with the powdered sample put on an aluminum sample holder. Next, phase identification was looked into.

2.3.2 High Resolution TEM

The samples were studied using Zeiss Auriga HRTEM to understand their morphology and structure. After the synthesized sample (0.02 g) was completely dispersed, it was floated in 10 cm^3 of methanol and ultrasonicated. Using a micropipette, two drops of the nanosuspension were applied to a perforated carbon lattice. Later, this was exposed to photo light to dry.

2.3.3 High Resolution SEM and EDS

Zeiss Auriga HRSEM in conjunction with EDS was deployed to examine the morphologies of the nanomaterials. Using the Quorum T15OT Analyzer, the sample (0.05 mg) was spread on carbon adhesive tape and sputter-coated with Au-Pd in five mins. After the coated sample was placed within the sample holder, imaging was performed at 5 kV with a high electron tension. The constituent elements of the samples were ascertained by operating the EDS at EHT for 20 kV, which is how the constituting elements of the materials were found.

2.3.4 Brunauer-Emmett-Teller (BET)

To eliminate any remaining water and volatile chemicals from the samples, a predefined mass (0.1 g) was first degassed for four hours at 95 °C. Plotting volume adsorbed against relative pressure yielded the BET surface area and pore size spread. Using Scherrer Debye equation (Eq 2), average crystallite size was calculated using total width at half maximum of the corresponding anatase peak. An acidic medium yielded the smallest confirmed crystallite size (Table 2: run 19).

$$D = \frac{k\lambda}{\beta \cos\theta} \tag{2}$$

where D is crystallite size, k represents shape factor (0.94), λ signifies wavelength of the X-ray source, and β is the full width at half maximum (FWHM). Fig 2 illustrates the crystallite sizes of some selected TiO_2 at varied runs.

3. Results and Discussion

3.1 Characterization of Optimized Materials and Their Nanocomposites via XRD

Tables 1 and 2 display the factorial design of 2^4 factorials and experimental runs, which were utilized to examine the impact of synthesis parameters on NP yield, including mixing duration, pH, precursor size, and volume of the extract. Cu Kα radiation was used as the X-ray source for the XRD examination, which yielded the crystallite size of the investigated TiO_2. As shown in Fig 3, the phase configuration according to estimated peak intensities was anatase.

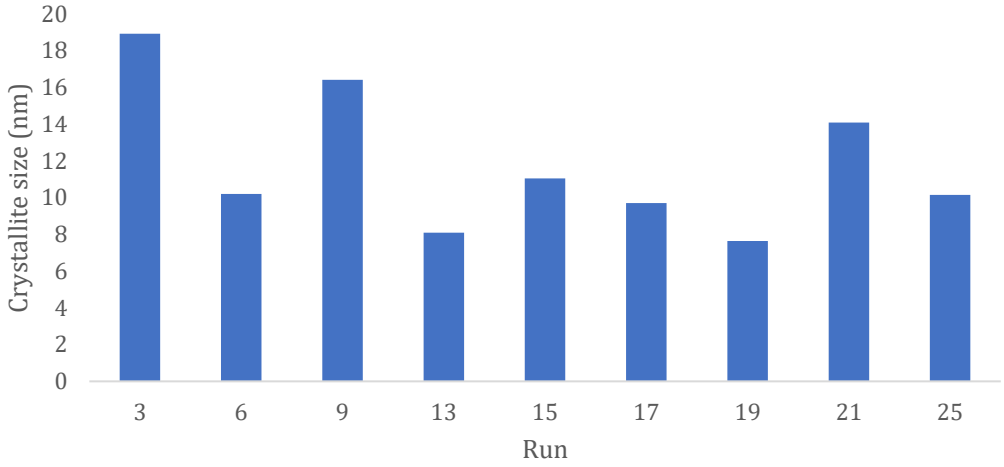

Fig. 2. Crystallite size of selected TiO2 at varied runs

The XRD data of individual material and their composites at various ratios of compounding are illustrated in Fig 3. The patterns indicate that TiO_2 is primarily composed of anatase peaks at 2θ = 25.2°, 37.7°, 48°, and 54°. Because of the anatase phase's enormous surface area, surface chemistry, and redox characteristics, catalytic activities occur there [31]. The XRD patterns of CNTs are displayed in Fig 4, which indicates that the sample exhibits two distinct peaks at approximately 31.6° and 52.1°. These peaks are indexed to the graphite reflections of (002) and (100), respectively. The peaks attributed to CNTs are hardly visible for the TiO_2/CNTs NCs (see Fig 4(A)), but anatase peaks are readily detected [31].

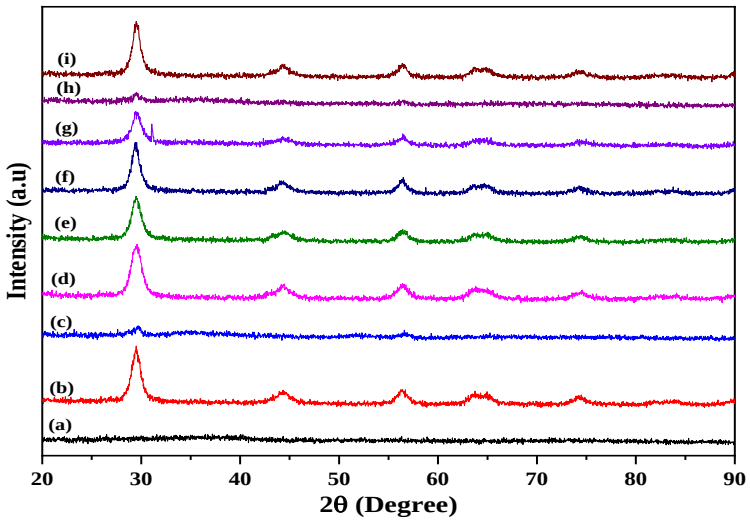

Fig. 3. XRD of TiO2 NPs for runs in Table 2

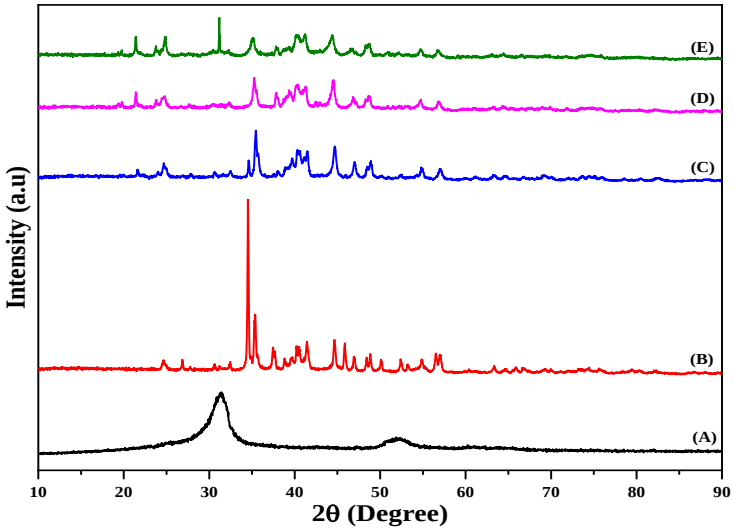

Fig. 4. XRD of CNTs (A), TiO2 (B), TiO2/CNTs (9:1; 7:3; 5:5)

The possible cause of this scenario could be the overlap between the TiO_2 and CNT major peaks. This could also be explained by low concentration of CNTs and the strong intensity of TiO_2 peaks. Notably, with CNTs, the breadth of the XRD peaks at 35.03° and 57.5° was somewhat widened. This procedure suggests significant alteration of the crystalline size of TiO_2-based NCs by the addition of CNTs.

3.2 HRSEM of Individual Materials and Their Nanocomposites

HRSEM pictures of individual materials and their nanocomposites at various ratios are shown in Fig 5. TiO_2 NPs form a fleck-like structure in Fig 5(a) and alternatively, Fig 5(b) reveals HRSEM image of tube-like CNTs with diameters ranging from 20 to 30 nm. The magnified images in Fig 5(c-e) establish uniform distribution of TiO_2 NPs on the reactive sites provided on the treated CNTs surfaces. CNTs are hardly identified in consistency with the NC's content ratios, prompting homogeneous dispersion of TiO_2 on CNTs in the NC (9:1) as seen in Fig 5(c). When comparing the TiO_2 NPs and their NCs, the HRSEM picture of the NPs shows gaps or voids which may indicate inter-particulate porosity. The morphologies observed for the NCs could have resulted from the intermolecular interaction between TiO_2 and defect sites on the surface of the CNTs.

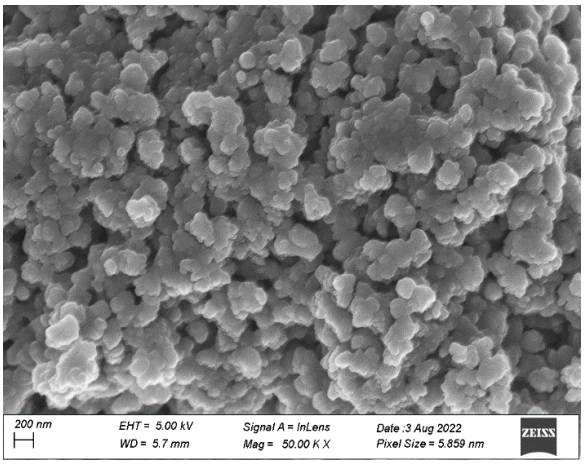

(a)

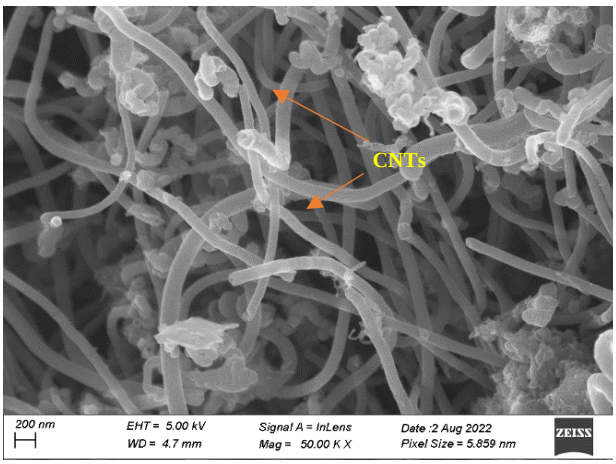

(b)

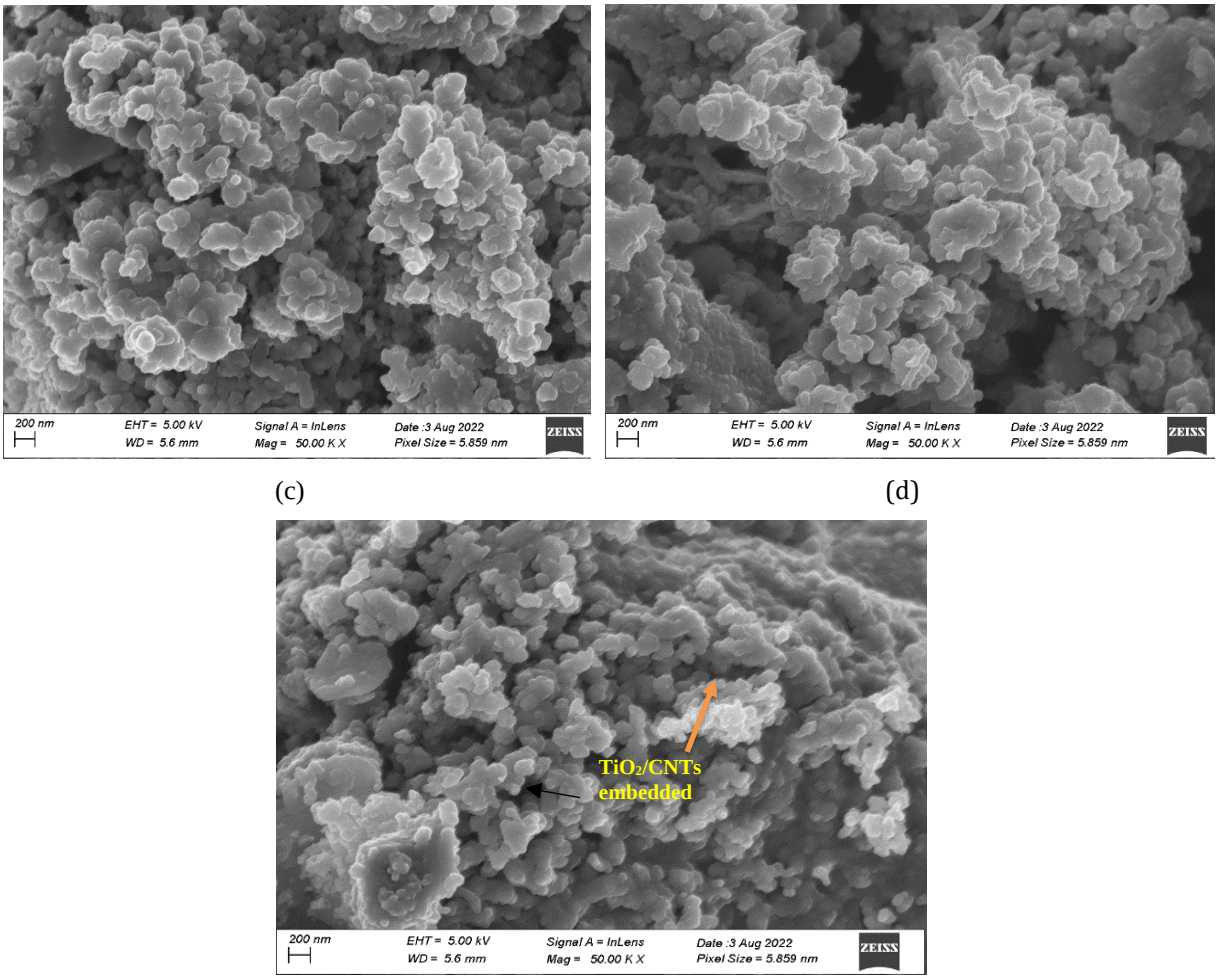

Fig. 5. (a) HRSEM pictures of TiO_2, (b) CNTs, (c)TiO_2/CNTs (9:1), (d) (7:3), and (e) (5:5)

3.3 HRTEM of Individual Materials and Their Nanocomposites

HRTEM pictures of TiO_2, CNTs, and varied NCs ratios are shown in Fig 6. The TiO_2 NPs are clearly spherical, as shown in Fig 6(a), and the CNTs that are formed are multi-walled, hollow, and have several inner diameters, as seen in Fig 6(b). The HRTEM pictures of NCs illustrated in Fig 6(c-e) show homogeneous dispersion with separate CNTs coated in TiO_2 and no aggregates between the TiO_2 and CNTs that resemble jams. While the TiO_2 distribution of the NCs steadily decreases, the mean size distribution of TiO_2 is 14.02 nm. The joining of the titania's hydroxyl group with the surface chemical groups of the CNTs may have caused this event by creating additional reaction sites during the CNTs' acid pretreatment. The visible locations of grain development for nanoparticles in the NCs are the surface flaws on the CNTs. On the other hand, as Fig 6(e) illustrates, adding more CNTs to TiO_2/CNTs NCs may decrease the magnitude of the crystallized TiO_2 on the CNTs and hence prevent the agglomeration of TiO_2 NPs. The polycentric ring of TiO_2 as witnessed in the EDS spectra is supported by the diffraction for anatase; nonetheless, the corresponding SAED patterns are characteristic of MWCNTs (Fig 7). The XRD analysis verified these as well. Additionally, the NCs exhibit polycentric rings with various reflection planes that resemble titania distributed in carbon nanotubes and create Ti-O-C and Ti-O-Ti networks. Ti, C, and O are the main constituents of the NCs, according to the EDS spectra (Fig 6), along with trace elements from kaolin catalysts and Ni salt. The Ti content in the composed NCs came after the mass ratio of the composites, according to the EDS study.

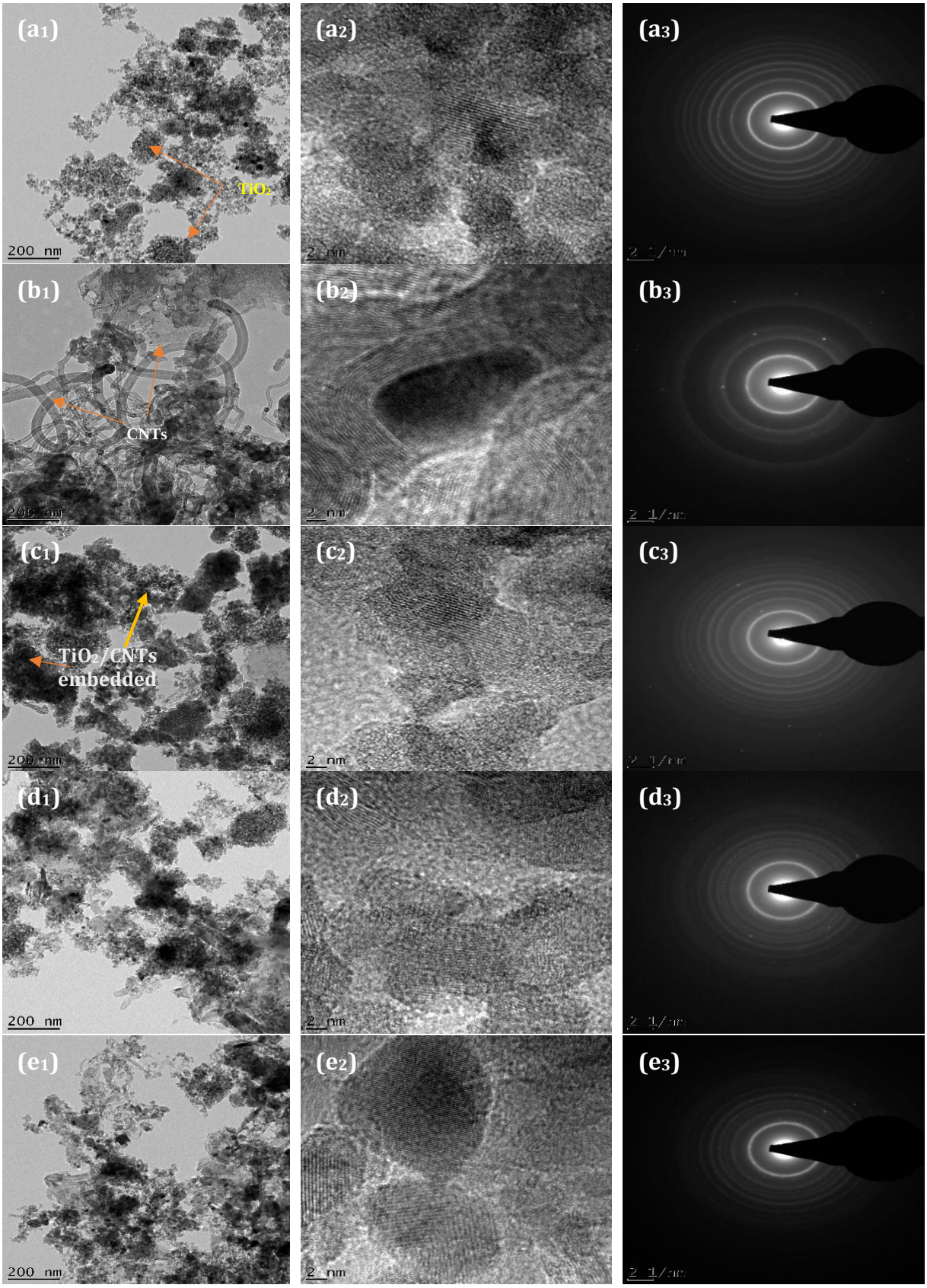

Fig. 6. (a) HRTEM images of TiO_2, (b)CNTs, (c)TiO_2/CNTs (9:1), (d) TiO_2/CNTs (7:3), (e)TiO_2/CNTs (5:5)

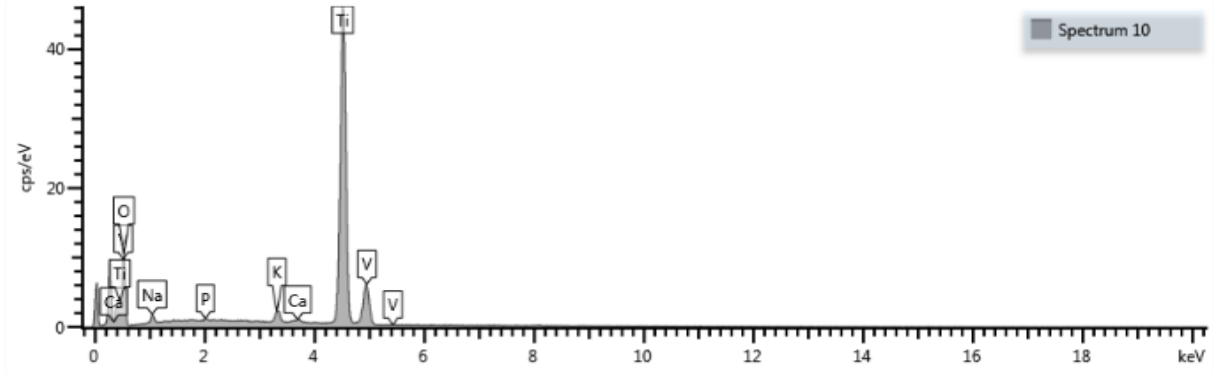
Spectrum 10
cps/eV
keV
O
Ti
Ca
Na
P
K
Ca
Ti
V
V

(a)

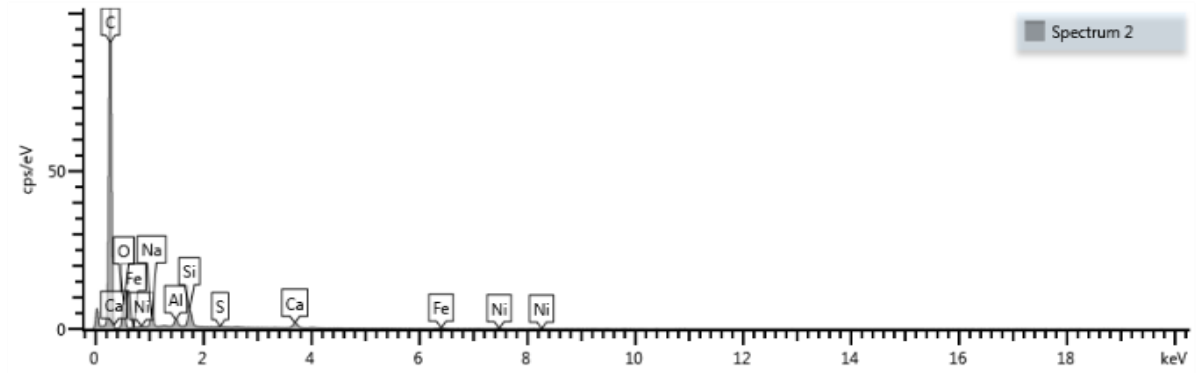
Spectrum 2
cps/eV
keV
C
O
Na
Fe
Si
Ca
Ni
Al
S
Ca
Fe
Ni
Ni

(b)

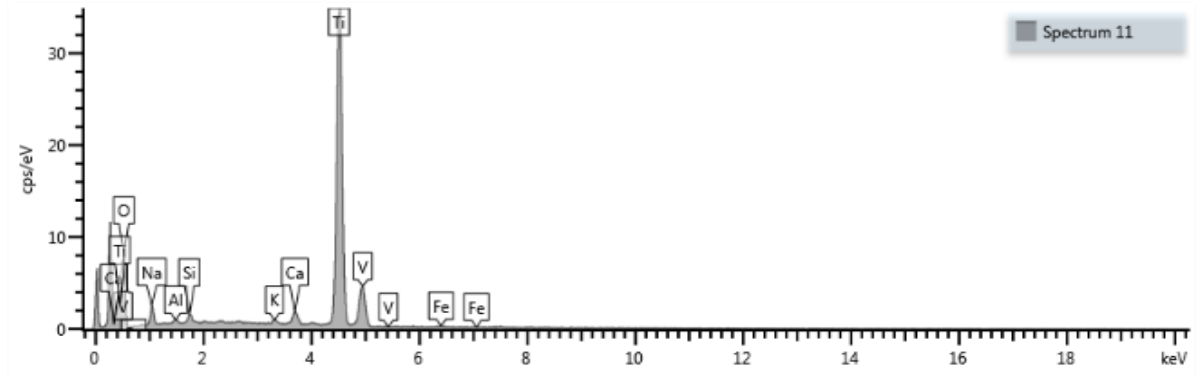
Spectrum 11
cps/eV
keV
Ti
O
Ti
Ca
Na
Si
V
Al
K
Ca
V
V
Fe
Fe

(c)

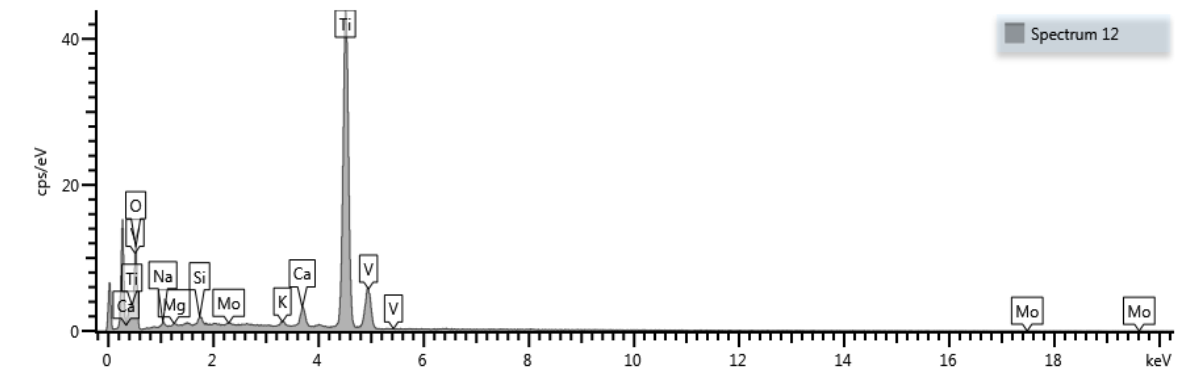
Spectrum 12
cps/eV
keV
Ti
O
V
Ti
Na
Si
Ca
Ca
Mg
Mo
K
V
V
Mo
Mo

(d)

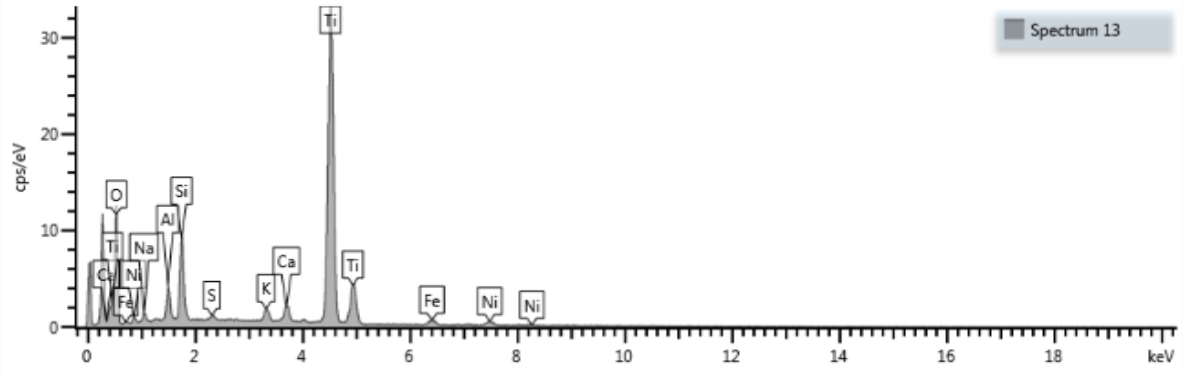

(e)

Fig. 7. (a)EDS results of TiO_2, (b)CNTs, (c)TiO_2/CNTs (9:1), (d) (7:3), (e) (5:5)

3.4 BET of Individual Materials and Their Nanocomposites

The N_2 adsorption-desorption isotherms of CNTs, TiO_2, and NCs are displayed in Fig 8, and Table 3 displays the BET-specific surface area, pore size, and pore volume. It is possible to identify the isotherms as intermediate cases between hysteresis loops of type I, where the two branches are almost vertical and parallel of a range of gas uptake, and type IV, where the branches stay virtually horizontal and parallel over a wide P/Po range, owing to the N_2 adsorption-desorption isotherm of TiO_2 [32]. The isotherm recognized for CNTs is type III isotherm (Fig 8(a)).

Table 3. Summary of BET results of individual materials and their nanocomposites

Sample	Surface area (m^2/g)	Pore size (nm)	Pore volume (cc/g)
CNTs	0.65	16.79	0.00276
gTiO_2	127.62	6.648	0.296
CNTs/gTiO_2 (1:9)	57.84	7.637	0.155
CNTs/gTiO_2 (3:7)	71.19	8.412	0.195
CNTs/gTiO_2 (5:5)	103.42	7.451	0.259

Type II isotherms, which can be linked to the merger of type I and type IV loops, are the isotherms originating from the NCs [33]. This can be explained by the fact that, in comparison to both TiO_2/CNTs (9:1) and TiO_2/CNTs, the isotherm shown in Fig 8(e) is closer to type II. The nanomaterials' BET surface areas are shown in Table 3. Compared to CNT, TiO_2 has a much bigger surface area, which suggests superior textural qualities and a greater variety of uses. Additionally, as TiO_2 falls in relation to the samples' CNT concentrations, the NCs' surface areas rise. The severing of TiO_2 NPs brought on by the inclusion of CNTs may be responsible for these phenomena. Moreover, mesoporous nanomaterials that may facilitate mass transfer are reflected in the pore sizes [34]. The NCs' pore volume increased as the CNT concentration increased, following the same trend as the surface area. This is understood by TiO_2's continuous filling of the reaction sites on CNT walls, according to previous study by Medupin et al. [35].

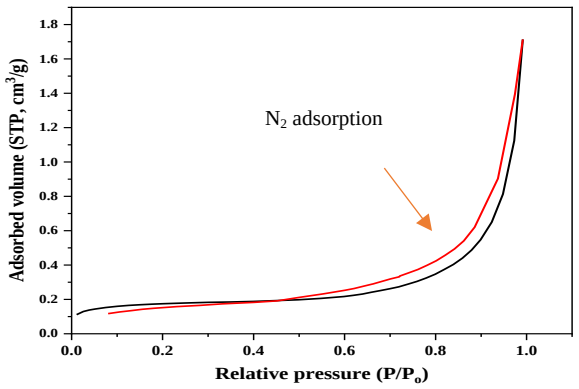

(a)

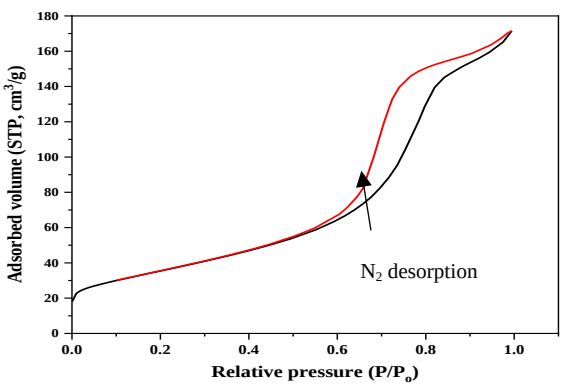

(b)

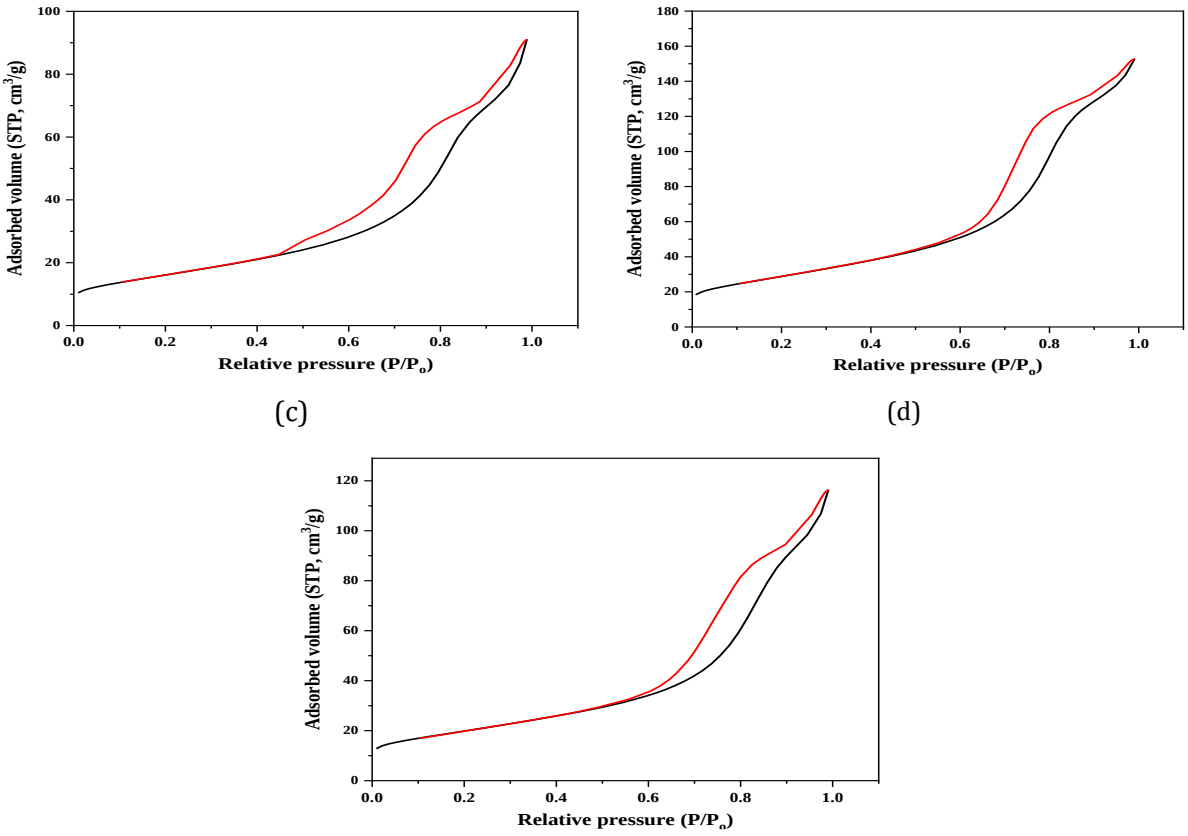

Fig. 8. (a)N_2 Adsorption-desorption curves of CNTs, (b)TiO_2, (c)TiO_2/CNTs (9:1), (d) (7:3), (e) (5:5)

3.5 FTIR of Separate Materials and Their Nanocomposite

FTIR helps to detect the characteristic vibration of chemical bonds between atoms of the nano components. Specific functional groups that indicate the presence and type of bonding in the nanocomposite can be identified by analyzing the adsorption peaks. The spectra in this research are recorded, then displayed in Fig 9. The bending vibration of adsorbed water molecules is responsible for the absorption at around 1630 cm^{-1} (Fig 9(a)).

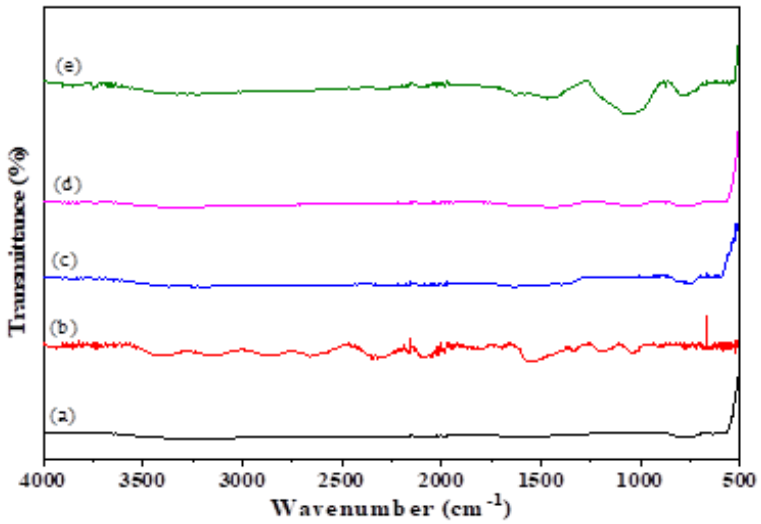

Fig. 9. (a)FTIR spectra of TiO_2, (b)CNTs, (c)TiO_2/CNTs (9:1), (d) (7:3), (e) (5:5)

The TiO_2 sample's broad band at 950 cm^{-1} is associated with the distinctive vibration of the Ti–O–Ti network. The CNTs (Fig 9(b)) exhibit C–C stretching bonds at 1650 cm^{-1}, which are identified as CNT modes. The peak at 1705 cm^{-1} is linked to the carboxyl group's C=O stretching, which is a feature of -COOH group [36–38]. The peaks at 3500–3300 cm^{-1} show a significant concentration of hydroxyl and carboxyl groups and correlate to their –OH stretching bonds. The composites include peaks consistent with C=C and Ti-O links, producing peaks allocated to Ti-O-C and C-O bonds, according to the FTIR spectra for the NCs, which are displayed in Fig 9(c, d, and e) [39]. These findings show that the growth produced a heterojunction at the gTiO_2 and CNT surfaces, creating interfacial connections in the matrices [34].

5. Conclusions

In conclusion, this research successfully synthesized and characterized green titania (TiO_2) and carbon nanotubes (CNTs) to develop TiO_2/CNTs nanocomposites with potential as hybrid nanofillers in nanofluids for machining carbon fiber reinforced plastics (CFRPs). Its findings demonstrate that carbon nanotubes (CNT) and green titania (TiO_2) nanocomposites could be dependable filler options for blending hybrid nanofluids for machining operations. After the analyses of the produced CNTs, TiO_2, and their NCs, it was discovered that the NPs were in good condition to be used as filler materials in both organic and inorganic base oils, for the creation of nanofluids intended for CFRP machining. The TiO_2 (particles) are observed to fill the sites formed after the CNTs (fibre) were purified and functionalized, which lessens the inherent difficulty of formulating the nanosuspension system. Three different nanofiller ratios were investigated under the same conditions, and it was found that adding fillers could significantly improve the stability of the nanofluids for machining application, with TiO_2/CNTs (7:3) NCs being the most stably dispersed of the three as could be noticed with the HRTEM micrographs. Agglomeration tendency, which has been identified by many earlier authors as the innate challenge with CNT system, is significantly reduced as TiO_2 nanoparticles occupy certain sites on the walls of the CNTs and break the van der Walls attractions between individual CNTs. The clustering merely shows that the TiO_2 in the suspension is drawn to the CNTs' wall apertures. However, the TiO_2/CNTs (5:5) NC has a distinct benefit over other NCs in that it could remove heat faster from the machining zone, according to the results of HRSEM/EDS, HRTEM, XRD, and BET. This is because it has the largest surface area for heat removal, the largest pore volume, and, indeed, the most stable nanosuspension of all the NCs studied in this research article. It is, therefore, anticipated that the hybrid nanosuspension that is produced after this study's successful synthesis, characterisation, and optimization will be useful as filler materials of improve the capacity of base oils to remove heat from cutting zones during machining operations. This work paves the way for further advancements in the use of nanocomposites in eco-friendly machining fluids, with broader implications for sustainable industrial practices.

Acknowledgement

The authors thankfully recognize the funding received from the TETFund, Nigeria, through the NRF with grant number: TETF/ES/DR&D/CE/NRF2020/SETI/113/VOL.1 for funding this research.

References

[1] Zheng H, Zhang W, Li B, Zhu J, Wang C, Song G, Wu G, Yang X, Huang Y, & Ma L. Recent advances of interphases in carbon fiber-reinforced polymer composites: A review, Composites Part B: Engineering, 2022;233, https://doi.org/10.1016/j.compositesb.2022.109639

[2] Erturk AT, Yarar E, Vatansever F, Sahin AE, Kilinçel M, & Alpay YO. A comparative study of mechanical and machining performance of polymer hybrid and carbon fiber epoxy composite materials, Polymer & Polymer Composites, 2021;29(9):S655–S666. https://doi.org/10.1177/09673911211020620

[3] Binali R, Ribeiro da Silva RR, Limenov DY, Kuntoglu M, Machado AR, Linul E. A review of progress trends of machining of carbon fibre reinforced plastics, Journal of Materials Research and Technology, 2024; In Press, https://doi.org/10.1016/j/jmrt.2024.10.050

[4] Elgnemi TSM, Jun MBG, Songmene V, & Samuel AM. Milling performance of CFRP composite and atomised vegetable oil as a function of fibre orientation, Materials, 2021;14(8), https://doi.org/10.3390/ma14082062

[5] Wang JJ, Zhang JF, Feng PF, & Guo P. Damage formation and suppression in rotary ultrasonic machining of hard and brittle materials: A critical review, Ceramics International, 2018;44(2): 1227–239, https://doi.org/10.1016/j.ceramint.2017.10.050
[6] Zhang MJ, et al. Analysis of flow field in cutting zone for spiral orderly distributed fibre tool, International Journal of Advances in Manufacturing Technology, 2017;92(9–12), 4345-354
[7] Lawal SA, Medupin RO, Yoro KO, Okoro UG, Adedipe O, Abutu J, Tijani JO, Abdulkareem AS, Ukoba K, Ndaliman MB, Sekoai PT, & Jen T-C. Nanofluids and their application in carbon fibre reinforced plastics: A review of properties, preparation, and usage, Arabian Journal of Chemistry, 2023;16(8):104908, https://doi.org/10.1016/j.arabjc.2023.104908
[8] Lawal SA, Medupin RO, Yoro KO, Ukoba KO, Okoro UG, Adedipe O, Abutu J, Tijani JO, Abdulkareem AS, Ndaliman MB, Abdulrahman AS, Eterigho-Ikelegbe O, Jen T-C. Nano-titania and carbon nanotube-filled rubber seed oil as machining fluids, Materials Chemistry & Physics, 2024;316:129126, https://doi.org/10.1016/j.matchemphys.2024.129126
[9] Medupin RO, Ukoba K, Yoro KO, & Jen T-C, Sustainable approach for corrosion control in mild steel using plant-based inhibitors: A review, Materials Today Sustainability, 2023;22:100373, https://doi.org/10.1016/j.mtsust.2023.100373
[10] Patole PB, Pol GJ, Desai AA, & Kamble SB. Analysis of surface roughness and cutting force under MQL turning using nano fluids, Materials Today: Proceedings, 2021;45:5684–688, https://doi.org/10.1016/j.matpr.2021.02.501
[11] Ni J, Cui Z, Wu C, Sun J, & Zhou J. Evaluation of MQL broaching AISI 1045 steel with sesame oil containing nano-particles under best concentration, Journal of Cleaner Production, 2021;320(May):128888, https://doi.org/10.1016/j.jclepro.2021.128888
[12] Haq MA, Hussain S, Ali MA, Farooq MU, Mufti NA, Pruncu CI & Wasim E. Evaluating the effects of nano-fluids based MQL milling of IN718 associated to sustainable productions, Journal of Cleaner Production, 2021;310(May):127463, https://doi.org/10.1016/j.jclepro.2021.127463
[13] Iruj M, Yaqoob S, Ghani Ja, Jaber H, Saibani N, Alkhedher M. State-of-the-art hybrid lubrication (cryo-MQL) supply systems, performance evaluation, and optimization studies in various machining process, Results in Engineering, 2024;22:102090.
[14] Usha M, & Srinivasa Rao G. Optimisation of Parameters in Turning Using Herbal Based Nano Cutting Fluid with MQL, Materials Today: Proceedings, 2019;22:1535-544 https://doi.org/10.1016/j.matpr.2020.02.115
[15] Agrawal SM, & Patil NG. Experimental study of non-edible vegetable oil as a cutting fluid in machining of M2 Steel using MQL, Procedia Manufacturing, 2018;20: 207–212, https://doi.org/10.1016/j.promfg.2018.02.030
[16] Gao T, Zhang Y, Li C, Wang Y, An Q, Liu B, Said Z, & Sharma S. Grindability of carbon fiber reinforced polymer using CNT biological lubricant, Scientific Reports, 2021;11(1);1–14, https://doi.org/10.1038/s41598-021-02071-y
[17] Singh Y, Negi P, Yadav A, & Tripathi R. Euphorbia lathyris: A novel feedstock for bio based lubricant application with titanium dioxide nanoparticles as additives, Materials Today: Proceedings, 2021;46;10518–522, https://doi.org/10.1016/j.matpr.2020.12.1237
[18] Zhang Y, Li L, Cui X, An Q, Xu, P, Wang W, Jia D, Lui M, Dambata YS, Li C. Lubricant activity enhanced technological for sustainable machining: Mechanisms and processability, Chinese Journal of Aeronautics, 2024; In Press, https://doi.org/10.1016/j.cja.2024.08.034
[19] Kumar A, Sharma AK, & Katiyar JK. State-of-the-art in sustainable machining of different materials using nano minimum quality lubrication (NMQL), Lubricants, 2023;11(64), https://doi.org/10.3390/lubricants11020064
[20] Bai X, Li C, Dong L, & Yin Q. Experimental evaluation of the lubrication performances of different nanofluids for minimum quantity lubrication (MQL) in milling Ti-6Al-4V, International Journal of Advances in Manufacturing Technology, 2019;101:2621–632
[21] Osman KA, Yılmaz V, Ünver HO, Seker U, & Kılıç, S. Slot milling of titanium alloy with hexagonal boron nitride and minimum quantity lubrication and multi-objective process optimization for energy efficiency, Journal of Cleaner Production, 2020;258:120739.
[22] Jamil MKhan AM, & Hegab H. Milling of Ti–6Al–4V under hybrid Al2O3-MWCNT nanofluids considering energy consumption, surface quality, and tool wear: A sustainable machining, International Journal of Advances in Manufacturing Technology, 2020;107:4141–4157
[23] Cui X, Li C, Ding W, Chen Y, Mao C, Xu X, Liu B, Wang D, Li HN, Zhang Y, Said Z, Debnath S, Jamil M, Ali HM, & Sharma S. Minimum quantity lubrication machining of aeronautical materials using carbon group nanolubricant: From mechanisms to application. Chinese Journal of Aeronautics, 2021;September. https://doi.org/10.1016/j.cja.2021.08.011
[24] Venkatesan K, Devendiran S, Sachin D, & Swaraj J. Investigation of machinability characteristics and comparative analysis under different machining conditions for sustainable manufacturing, Measurement:

Journal of International Measurement Confederation, 2020;154:107425, https://doi.org/10.1016/j.measurement.2019.107425
[25] Shokrani A, Arrazola PJ, Biermann D, Matevenga P, Jawahir IS, Sustainable machining: recent technological advances, CIRP Journal of Manufacturing Sciences and Technology, https://doi.org/10.1016/cirp.2024.06.001
[26] Gao T, et al. Surface morphology assessment of CFRP transverse grinding using CNT nanofluid minimum quantity lubrication, Journal of Cleaner Production, 2020;277:123328. https://doi.org/10.1016/j.jclepro.2020.123328
[27] Abubakre OK, Medupin RO, Akintunde IB, Tijani JO, Abdulkareem AS, Muriana RA, James JA, Ukoba KO, Jen T-C, & Yoro KO. Carbon nanotube-reinforced polymer nanocomposites for sustainable biomedical applications: A review, Journal of Science: Advanced Materials and Devices., 2023;8(2):100557, https://doi.org/10.1016/j.jsamd.2023.100557
[28] Urmi WT, Shafiqah AS, Rahman MM, Kadirgama K, & Maleque MA. Preparation Methods and Challenges of Hybrid Nanofluids: A Review, Journal of Advanced Research in Fluid Mechanics and Thermal Sciences, 2021;78(2):56–66, https://doi.org/10.37934/ARFMTS.78.2.5666
[28] Medupin RO, Abubakre OK, Abdulkareem AS, Muriana RA, & Abdulrahman AS. Carbon Nanotube Reinforced Natural Rubber Nanocomposite for Anthropomorphic Prosthetic Foot Purpose, Scientific Reports, 2019;9(1):20146, https://doi.org/10.1038/s41598-019-56778-0
[28] Ma C, Wen R, Zhou F, Zhao H, Bao X, Evelina A, Long W, Wei Z, Ma L, Liu J, & Chen S. Preparation and application of an environmentally friendly compound lubricant based biological oil for drilling fluids, Arabian Journal Chemistry, 2022;15(3):103610, https://doi.org/10.1016/j.arabjc.2021.103610
[28] Mustapha S, Ndamitso MM, Abdulkareem AS, Tijani JO, Shuaib DT, Ajala AO, & Mohammed AK. Application of TiO2 and ZnO nanoparticles immobilized on clay in wastewater treatment: a review, Applied Water Science, 2020;10(1), https://doi.org/10.1007/s13201-019-1138-y
[28] D'Aloia AG, Di Fransesco A, & De Santis V. A novel computational method to identify/analyses hysteresis loops of hard magnetic materials, Magnetochemistry, 2021;7(10).
[28] Brockmann EC, Pyykko M, Hannula H, Khan K, Lamminmaki U, & Huovinen T. Combinatorial mutagenesis with alternative CDR-L1 and H2 loop lengths contributes to affinity maturation of antibodies, New Biotechnology, 2020;60:73-182
[28] Paumo HK, Dalhatou S, Katata-Seru LM, Kamdem BP, Tijani JO, Vishwanathan V, Kane A, & Bahadur I. TiO2 assisted photocatalysts for degradation of emerging organic pollutants in water and wastewater, Journal of Molecular Liquids, 2021;331:115458, https://doi.org/10.1016/j.molliq.2021.115458
[28] Medupin RO, Abubakre OK, Abdulkareem AS, Muriana RA, & Lawal SA. Dimensional and Thermal Reliability of Multi-Walled Carbon Nanotube Filled Natural Rubber Nanocomposites, International Journal Engineering Resources in Africa, 2020;51:177-189, https://doi.org/10.4028/www.scientific.net/jera.51.177
[28] Medupin RO, Abubakre OK, Abdulkareem AS, Muriana RA, Kariim I, & Bada SO. Thermal and physico-mechanical stability of recycled high-density polyethylene reinforced with oil palm fibres, Engineering Science & Technology, an International Journal, 2017;20(6):1623–631, https://doi.org/10.1016/j.jestch.2017.12.005
[28] Gopiraman M, Selvakumaran N, Kesavan D, Kim IS, & Karvembu R. Chemical and physical interactions of 1-benzoyl-3,3-disubstituted thiourea derivatives on mild steel surface: Corrosion inhibition in acidic media, Industrial & Engineering Chemical Research, 2012;51(23):7910–7922, https://doi.org/10.1021/ie300048t
[28] Shaban MM, Eid AM, Farag RK, Negm NA, Fadda AA & Migahed MA. Novel trimeric cationic pyrdinium surfactants as bi-functional corrosion inhibitors and antiscalants for API 5L X70 carbon steel against oilfield formation water, Journal Molecular Liquids, 2020;305:112817, https://doi.org/10.1016/j.molliq.2020.112817
[28] Khadom AA, Abd AN, Ahmed NA, Kadhim MM, & Fadhil AA. Combined influence of iodide ions and Xanthium Strumarium leaves extract as eco-friendly corrosion inhibitor for low-carbon steel in hydrochloric acid, Current Research in Green and Sustainable Chemistry, 2022;5(December):100278, https://doi.org/10.1016/j.crgsc.2022.100278